Effect of metallic silver nanoparticles on the alignment and relaxation behaviour of liquid crystalline material in smectic C* phase

Tripti Vimal,[1] Swadesh Kumar Gupta,[2] Rohit Katiyar,[1] Atul Srivastava,[1] Michal Czerwinski,[3] Katarzyna Krup,[3] Sandeep Kumar,[4] and Rajiv Manohar[1,a)]
[1]*Liquid Crystal Research Laboratory, Department of Physics, University of Lucknow, Lucknow 226007, India*
[2]*Experimental Quantum Interferometry and Polarization Group, Physics Department, IIT Delhi, Delhi 110016, India*
[3]*Institute of Chemistry, Military University of Technology, 00-908 Warsaw, Poland*
[4]*Soft Condensed Matter Laboratory, Raman Research Institute, Bangalore 560080, India*

(Received 31 March 2017; accepted 2 September 2017; published online 19 September 2017)

The influence of silver nanoparticles dispersed in a Ferroelectric Liquid Crystal (FLC) on the properties of the resultant composite system has been investigated by thermal, electro–optical, and dielectric methods. We show that the concentration of thiol capped silver nanoparticles is a critical factor in governing the alignment of nanoparticles (NPs) in the host FLC. The orientation of NPs in composite samples affects the ordering of the LC (Liquid Crystal) phase and consequently changes the various phase transition temperatures of the host LC. Formation of self-assembled 2D (two dimensional) arrays of nanoparticles is observed for high concentration of dopant in the LC, oriented perpendicular to the direction of rubbing. We propose that the molecular interaction between the thiol capped NPs and LC molecules is the key factor behind such an arrangement of NPs. Orientation of NPs has affected the relaxation behaviour and various other material parameters, significantly. A noteworthy change in DC conductivity articulates our proposed idea of the formation of 2D array of NPs perpendicular to the direction of rubbing. This comprehensive study endorses the importance of dopant concentration in modifying the properties of the host LC material. *Published by AIP Publishing*. [http://dx.doi.org/10.1063/1.5003247]

I. INTRODUCTION

The development of nanotechnology provides new opportunities in the field of experimental research.[1,2] In recent years, hybrid systems consisting of nanoparticles (NPs) and organic materials have emerged as an active area of research for advanced future materials and applications.[3,4] Liquid crystals (LCs) are fascinating organic materials being unique in their properties such as directional anisotropy and fluidity like ordinary liquids.[5] Efforts have been made to improve the properties of LCs by dispersion of nanoparticles,[6–8] polymer,[9,10] dye,[11] carbon nanotubes (CNTs),[12,13] nanorods,[14] and quantum dots.[15] Nanoparticle dispersed LC composites are useful in electro-optic devices based on LCs. Among all the Nanoparticles, Metal NPs have received much attention because of their excellent magnetic,[16] electronic,[17] and optical properties.[18] Metal NPs are very important because of their dipole particle plasmon resonance.[19] The qualitative analysis of dipole and quadrupole plasmon resonances shows the influence of the size, shape, and dielectric environment on the optical properties of metal NPs.[20] The localised surface plasmon resonance of metal NPs fall into the visible region, so these metal NPs are best tools for optical sensing of change in the refractive index. There such behaviour makes them useful for optical devices. The large anisotropy of the LC refractive index is ideally suited for tuning of the plasmon resonance by electric field-induced switching of the LC director orientation.[21] Several reports include the study of various properties of metal NPs and liquid crystal composites. The non-volatile memory effect based on a gold NP dispersed deformed helix ferroelectric liquid crystal (FLC) has been observed by Biradar *et al.*[22] The effect of Pd NPs on the electro optical features of the FLC (Ferroelectric Liquid Crystal) has been explored for futuristic device applications.[23] The enhancement of optical birefringence and electro-optical properties of nematic LCs with inclusion of gold NPs has been discussed by Vardanyan *et al.*[24,25] Discotic LCs have also shown significant improvement in various properties after the dispersion of a minute amount of metal NPs into them.[26,27] Some other studies also elaborate the changes in various parameters of the host LC material after the dispersion of different metal NPs.[28,29] Incorporation of metal NPs enhances not only the electro-optical properties of the LCs but it also affects the alignment of LC molecules.[30,31] The elastic-mediated interactions between the liquid crystalline medium and guest particles lead to the self-assembly of nanostructures.[32] These assemblies of nanostructures in LCs can be reoriented by external applied field. LCs are a unique candidate to guide the NP assembly, which is important for manipulating the spatial arrangement of NPs.[33]

In the present study, we have discussed the influence of metallic silver nanoparticles (Ag NPs) on the properties of the host multicomponent Ferroelectric Liquid Crystal mixture (W343). It has been observed in the Polarizing Optical Microscopy (POM) analysis that the local alignment of NPs in a planar aligned cell is highly dependent on the concentration of NPs. Formation of self-assembled 2D (two dimensional)

a)Author to whom correspondence should be addressed: rajiv.manohar@gmail.com. Tel.: (+91)9415000687. Fax: +91-522-26936.

arrays of nanoparticles in the perpendicular direction of rubbing has been observed in the planar aligned textures of composites having high dopant concentration [Mix.2 (0.3 wt./wt. % NPs in FLC) and Mix.3 (0.5 wt./wt. % NPs in FLC)]. These nanoparticle arrays influence the first order transition temperatures of the host FLC material, significantly. Changes in transition temperature have been confirmed by the thermal analysis of the composites. The effect of these 2D arrays of nanoparticles on the relaxation dynamics of the FLC material has been studied with the help of a dielectric spectroscopic technique. The non-appearance of the characteristic Goldstone mode (GM) in the SmC* phase of Mix.3 is very surprising. The electro-optical study has also been done to envisage about the polarizing ability of the composites and to support the outcomes of the dielectric analysis.

II. EXPERIMENTAL DETAILS

A. FLC material and nanoparticles

The FLC material (W343) has been used in the present study as a host material and it has been obtained from institute of chemistry, Warsaw Poland. It is a multicomponent mixture of fluorine substituted organic compounds with a chiral dopant. Silver nanoparticles have been used as the dopant material. The morphology of nanoparticles was characterized using HR-TEM (High Resolution-Transmission Electron Microscopy) and SEM (Scanning Electron Microscopy). The HR-TEM images confirm the homogeneous size distribution of silver nanoparticles.[34] Mostly, the metal nanoparticles are unstable in environment: coalescing, agglomerations, growing to large clusters, or etc., results. Also, they are intrinsically hydrophobic and tend to get aggregated in aqueous solution. The used silver nanoparticles are therefore capped with hexanethiol to reduce the possibility of self-aggregation. The average diameter of silver nanoparticles is about 2–4 nm. These NPs were further characterized using SEM which reveals uniform size distribution of nanoparticles. Silver NPs have been dispersed in chloroform for making the composites.

B. Preparation of LC sample cells and silver NPs/FLC composites

The LC sample cells were fabricated on the ITO (Indium Tin Oxide) coated glass plates by a photolithographic process. The dimension of the active area is 5 mm × 5 mm. For homogeneous alignment of molecules, a thin polyamide layer of nylon (6/6) has been deposited on these ITO patterned glass plates and then rubbed in an antiparallel way with the help of velvet cloth. The uniform cell thickness (6 μm in our case) was maintained by placing a mylar spacer. Three silver NPs/FLC composites were prepared by dispersing an appropriate amount of NPs into pure FLC material: Mix.1 (0.1 wt./wt. % NPs in FLC), Mix.2 (0.3 wt./wt. % NPs in FLC) and Mix.3 (0.5 wt./wt. % NPs in FLC). The composites were homogenized by an ultrasonic mixer for 1 h at 135 °C. The assembled cells were filled with pure FLC and NPs/FLC composites by capillary action, at 10 °C above the isotropic temperature of the FLC material. The cells were cooled gradually to room temperature. A polarizing optical microscope has been used to check the possibility of the formation of micro-aggregates of dopant in the cell.

C. Optical and thermal studies

The alignment of the pure FLC material and composites has been analyzed by the polarizing optical microscope (Radical instruments, RXLR-5) under the crossed polarizer-analyzer condition at RT (room temperature). The polarizing optical microscope interfaced with a CCD camera has been used for capturing the POMs.

A DSC (Differential Scanning Calorimetry) scan has been performed by a power compensated calorimeter using a NETZSCH DSC 200 F3 Maia in heating and cooling cycles with 2 °C/min heating/cooling rate.

D. Dielectric permittivity study

The dielectric parameters have been measured as a function of temperature by dielectric spectroscopy of the sample. A computer controlled impedance/gain phase analyser (Solartron SL1260) has been used for the same in the frequency range of 10 Hz–1 MHz.[35] In order to vary the temperature, a temperature controller (INSTEC HCS 302) has been used. A computer programme (WINTEMP) has been used to control the temperature of the temperature controller. The experiment was performed at a very slow heating rate, and the temperature was measured with an accuracy of ±00.1 °C.

E. Electro-optical measurements

An electro-Optical (E-O) setup has been used to visualize switching characteristics, spontaneous polarization, response time, and optical tilt angle values. It comprises: 5 mW He–Ne laser of 633 nm wavelength, a rotating stage, a function generator (Tektronix AFG-3021B), a digital oscilloscope (Tektronix TDS-2024C), a photo detector (Instec PD02-L1), and a heating stage attached with a temperature controller (INSTEC HCS 302). The Spontaneous Polarization (Ps) of the pure FLC material and silver NPs/FLC composites was obtained by a polarization current reversal method by applying a triangular wave of 52 Vpp at 10 Hz.[36] The optical tilt angle and optical response time measurements have been done at room temperature by applying 52 Vpp square wave pulse at 10 Hz to the planar aligned cell.[37]

III. RESULTS AND DISCUSSION

A. Differential scanning calorimetry (DSC) studies

Different phases [SmC* (chiral smectic C), SmA (smectic A), N* (Chiral nematic) and isotropic] of the LC material with their corresponding transition temperature can be established by the DSC at atmospheric pressure. Dispersion of nanoparticles affects the order parameter of the phases shown by the host LC material. A typical DSC curve shows various humps corresponding to the various phase transition temperatures. The DSC curves in heating cycles for pure FLC material, Mix.1, Mix.2, and Mix.3 are shown in Fig. 1. All samples were subjected to heating at a low scan rate of 2 °C/min. Suitable marking has been done to clearly visualize the

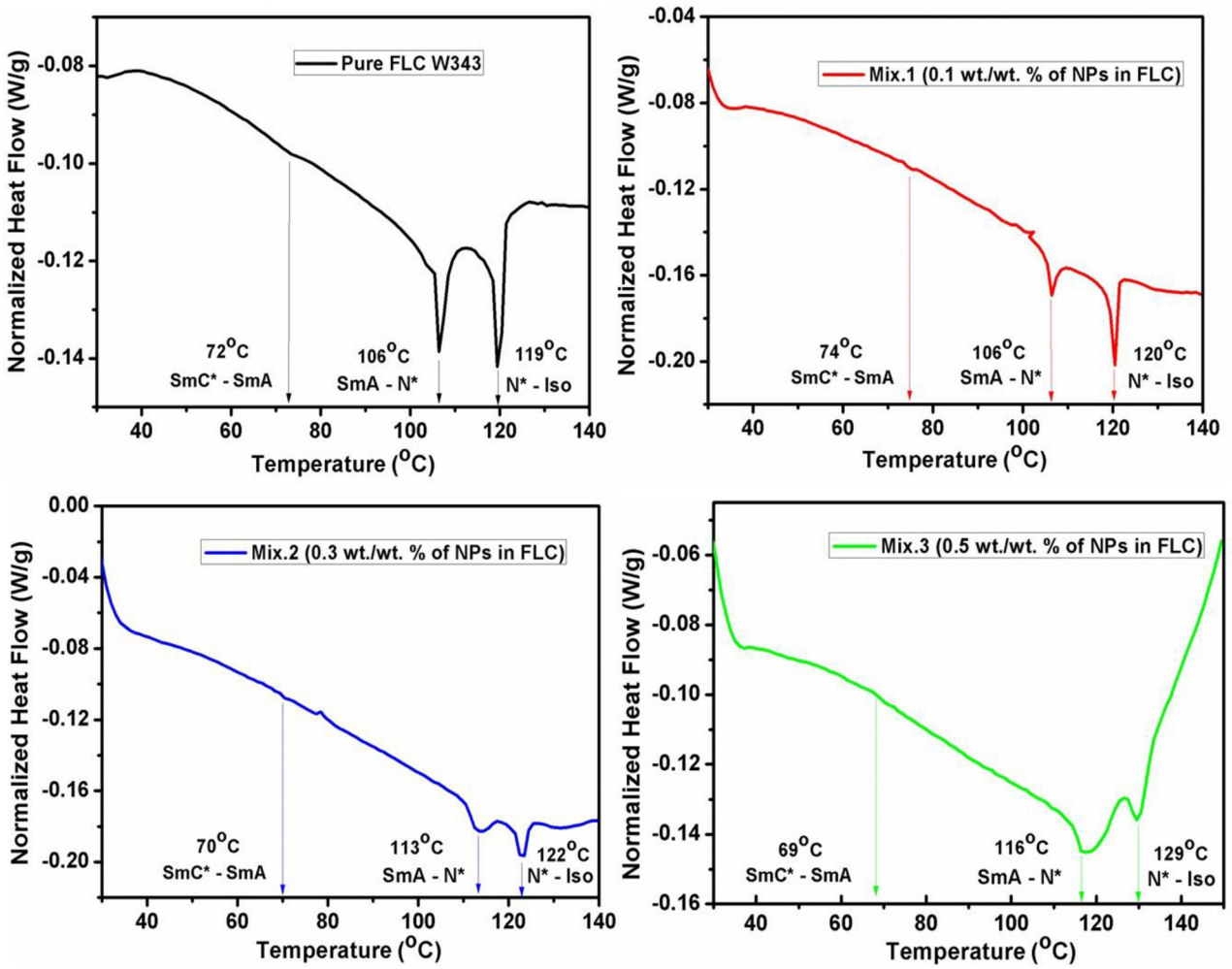

FIG. 1. Normalized differential scanning calorimetry (DSC) curves of pure FLC (W343) and NP dispersed FLC composites during the heating cycle. The DSC scan rate was 2 °C/min for all the samples.

change in transition temperature in the presence of silver nanoparticles. It can be seen that the DSC curve of the pure FLC material consists of two prominent peaks. Among them, the first large peak nearly at 106 °C is due to the SmA-N* phase transition and the second large peak at 119 °C corresponds to the N*-isotropic phase transition, respectively. A small deflection in the normalized heat flow has been observed near 72 °C. This small deflection in the normalized heat flow might be due to the change in the phase of the FLC material (from SmC*-SmA phase). Small variation in the normalized heat flow suggests that there is a very low change in the enthalpy value (delta H) during this phase transition.[38–40] The SmC*-SmA phase transition in the FLC is often a second order phase transition[41,42] and the second order phase transitions are generally not very sharp. It can be seen from the figure that the dispersion of a small quantity of nanoparticles (Mix.1) does not cause any noticeable change in the SmA-N* and N*-isotropic phase transition temperatures of the host FLC material except a very small increase in the SmC*-SmA phase transition temperature. Such behaviour of Mix.1 shows that the small concentration of NPs does not perturbs the helical structure of FLC. On the contrary, it increases the ordering of the SmC* phase due to the self-aligning nature of NPs in LCs. However, as dopant concentration is increased further in the FLC material (Mix.2 and Mix.3), change in all the phase transition temperatures can be observed [Fig. 1]. The SmC*-SmA is found to be slightly affected in the case of both the composites. As discussed in the subsequent POM analysis section, the formation of 2D arrays of nanoparticles between the smectic layers occurs for the composites having high dopant concentration. The 2D arrays of nanoparticles well adapted to the FLC layer arrangement disconnects the continuous helical structure in Mix.2 and Mix.3 and concurrently disturbs the helical geometry of the molecules. Therefore, the presence of 2D arrays of NPs affects the order of the SmC* phase adversely causing a decrement in SmC*-SmA phase transition temperature for both the composites.

The DSC traces of Mix.2 and Mix.3 are accompanied by the sharp and clearly visible peaks corresponding to SmA-N* and N*-Iso transition temperatures. The sharp peak indicates that they are first order in nature and has been shifted to the high temperature side with the broadening of the corresponding peaks for the composites (Mix.2 and Mix.3). It seems that the dispersion of NPs affects the coupling between the orders of the phases and consequently broadening of the two phase coexistence region occurs.[43] Broadening of the peaks envisages the delayed transformation of the phases into each other

in the composites. The SmA-N* and N*-Iso transition temperature has been increased by 7 °C and 3 °C for Mix.2. For Mix.3, both the phase transition temperatures have been increased by almost 10 °C. The thermal stabilization for the chiral nematic and smectic A phase has very surprizing and stimulating results. Typically, NPs dispersed in the chiral nematic (N*) and Smectic mixture show either no or destabilizing effect. It seems that the self-assembled 2D arrays of nanoparticles aligned between the smectic layers enhance the overall order parameter of the chiral nematic and smectic A phase. Such a drastic stabilizing effect has been described so far for inclusion of polar ferroelectric NPs and anisometric CNTs.[44,45] Phase stability increases with the concentration of nanoparticles in the host LC as it would lead to the formation of more and more 2D arrays of nanoparticles. In general we can say that formation of 2D arrays of nanoparticles perpendicular to the direction of rubbing causes a stabilizing effect for both the smectic and chiral nematic phase with the slight perturbation in the helical structure in the SmC* phase.[33]

B. POM (polarizing optical microscopy) image analysis

The polarizing optical microscopic study of composites (without any application of electric field) provides the information about the change in alignment of FLC molecules in the presence of NPs. They can be used to get the information about any aggregations and assemblies of NPs in the composite system. Figures 2, 3, 4, and 5 show the POM images (under crossed polarizer-analyzer condition) of pure FLC, Mix.1, Mix.2, and Mix.3, respectively, at different temperatures and different phases in the homogeneously aligned samples. Figure 2 provides the POM images of the FLC material (a) in deep SmC*, (b) near transition from the SmC*-SmA phase, (c) in the SmA phase, (d) near transition from the SmA-N* phase, and (e) in the N* phase. Figure 2(a) shows homogenously aligned texture for the SmC* phase. As the temperature increases, transition from the SmC*-SmA phase occurs and paramorphotic banded focal conic fan texture of SmA appears [Figs. 2(b) and 2(c), respectively].[46] With further increase in the temperature, the material changes its phase from SmA-N*. This phase transition is accompanied by the formation of large platelets of different colors, which finally leads to the plane texture of the cholesteric phase [Figs. 2(d) and 2(e), respectively]. Figure 3 represents the POM images of Mix.1 for all the phases. It can be observed that a small amount of NPs in the FLC material (Mix.1) improves the alignment of molecules in the SmC* phase. It is due to the self-aligning nature of NPs in LCs.[47] As a result, a small increase in the SmC*-SmA phase transition temperature occurs. This confirms the result observed for Mix.1 in the DSC analysis.

It is very interesting to observe large alignment changes in the POMs of Mix.2 and Mix.3 (Figs. 4 and 5). The aligned texture of the SmC* phase for Mix.2 is accompanied by the formation of self-assembled 2D arrays of nanoparticles perpendicular to the direction of the helical axis or the direction of rubbing. In between the two nearby assemblies, a well aligned texture of the SmC* phase has also been observed. In a planar aligned cell, the LC molecules are oriented along the rubbing direction due to the anchoring imposed by an alignment layer on electrodes and a small amount of guest particles generally tend to align in the same direction. However, in the present study this concept is not followed as we increase the dopant concentration from 0.1 to 0.3 wt./wt. %. So, it can be believed that with the increasing dopant concentration, the molecular interaction between the NPs and the LC molecules starts playing an important role. NPs are usually surface passivated with the help of a capping agent. In the present case, used NPs are stabilized by a monolayer

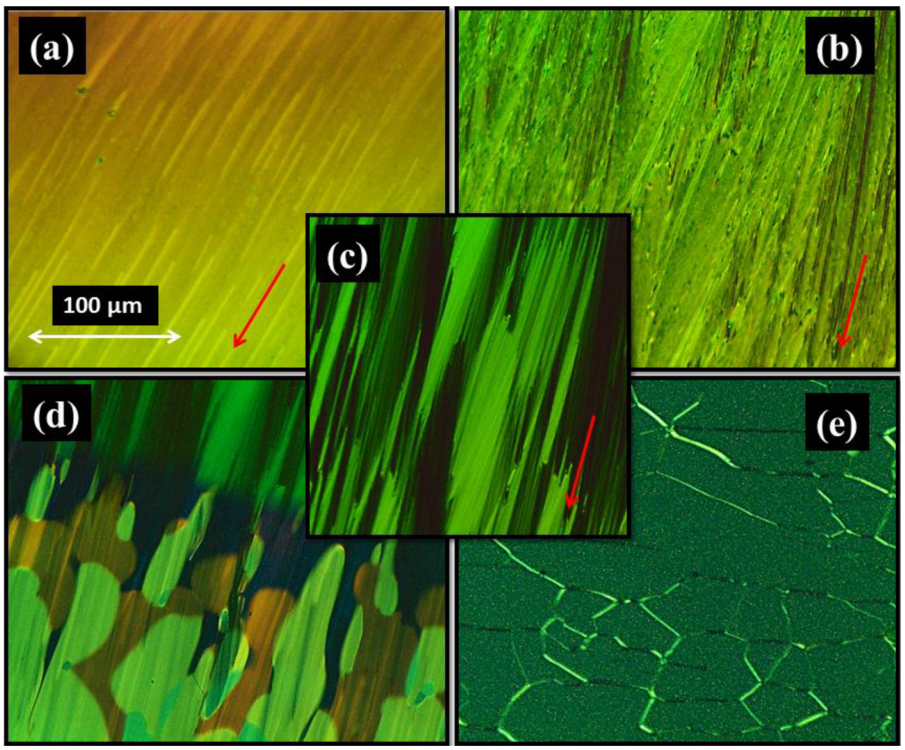

FIG. 2. Polarizing optical micrographs (under crossed polarizer-analyzer condition) of the pure FLC material during the entire mesogenic phase. (a) In the deep SmC* phase (at 35 °C), (b) near transition from the SmC*-SmA phase (71 °C), (c) In the SmA phase (at 100 °C), (d) near transition from the SmA-N* phase (at 105 °C), and (e) In the N* phase (at 116 °C). The scale bar is the same for all the POMs and the red arrow represents the direction of rubbing.

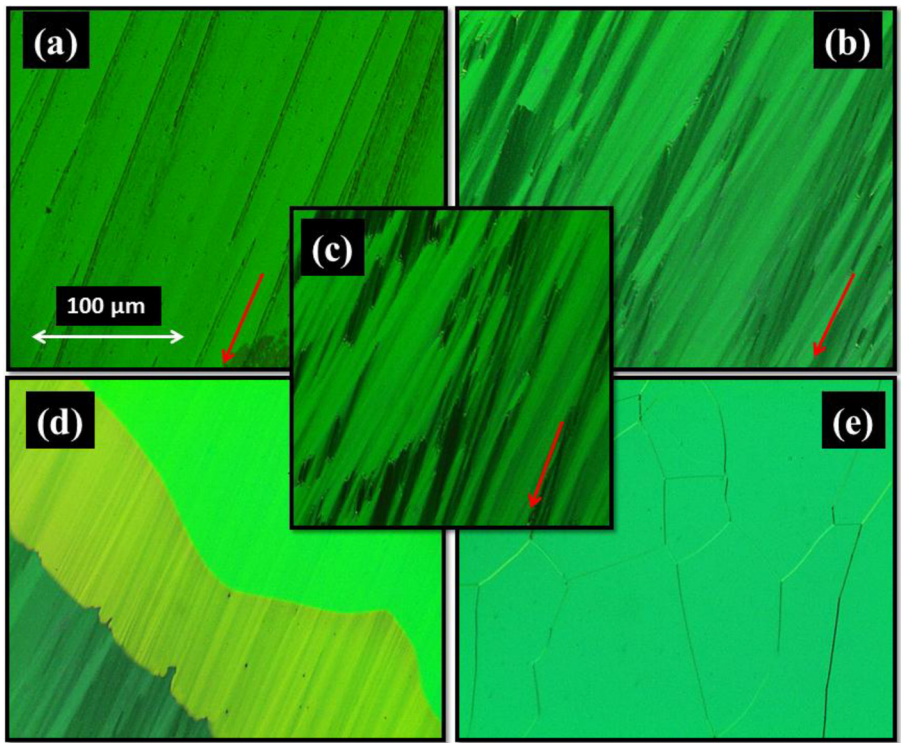

FIG. 3. Polarizing optical micrographs (under crossed polarizer-analyzer condition) of Mix.1 during the entire mesogenic phase. (a) In the deep SmC* phase (at 35 °C), (b) near transition from the SmC*-SmA phase (73 °C), (c) In the SmA phase (at 100 °C), (d) near transition from the SmA-N* phase (at 105 °C), and (e) In the N* phase (at 116 °C). The scale bar is the same for all the POMs and the red arrow represents the direction of rubbing.

of thiol ligands. The thiol ligand consists of a polar group and a non-polar aliphatic tail. They show hydrophilic and hydrophobic nature, respectively. The surface functionality of the NPs is defined by these non-polar aliphatic tails. Non covalent interaction between these aliphatic tails leads to the self-assembled arrangement of NPs. When dispersed in the LC, these self-assembled NPs usually align parallel to the rubbing direction due to strong anchoring conditions. Alignment of these self-assembled NPs between the smectic layers indicates that some kind of repulsive interaction is taking place in the system having higher dopant concentration.

The present FLC is a multicomponent mixture; a combination of dialkyldifluoroterphenyl organic achiral mesogenic compounds (in a certain percentage) with a chiral dopant. It is well known that in fluorine substituted organic compounds the fluorocarbon groups are hydrophobic in nature.[48] Hence in the present case, it might be possible that the hydrophobic fluorocarbon creates a repulsive force for the hydrophobic

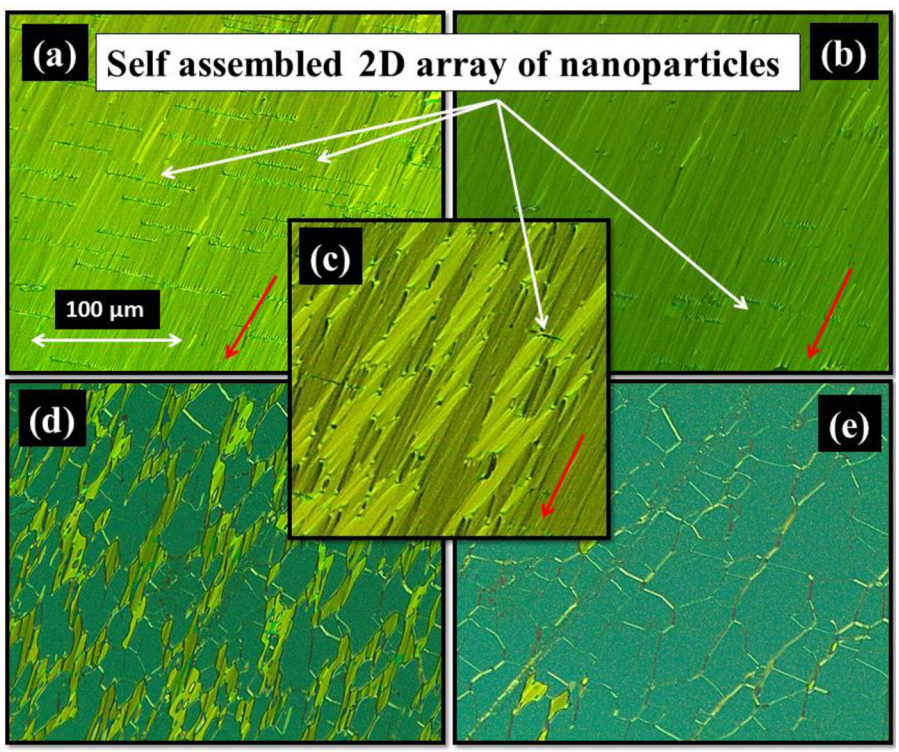

FIG. 4. Polarizing optical micrographs (under crossed polarizer-analyzer condition) of Mix.2 during the entire mesogenic phase. (a) In the deep SmC* phase (at 35 °C), (b) near transition from the SmC*-SmA phase (69 °C), (c) In the SmA phase (at 100 °C), (d) near transition from the SmA-N* phase (at 112 °C), and (e) In the N* phase (at 118 °C). The scale bar is the same for all the POMs and the red arrow represents the direction of rubbing.

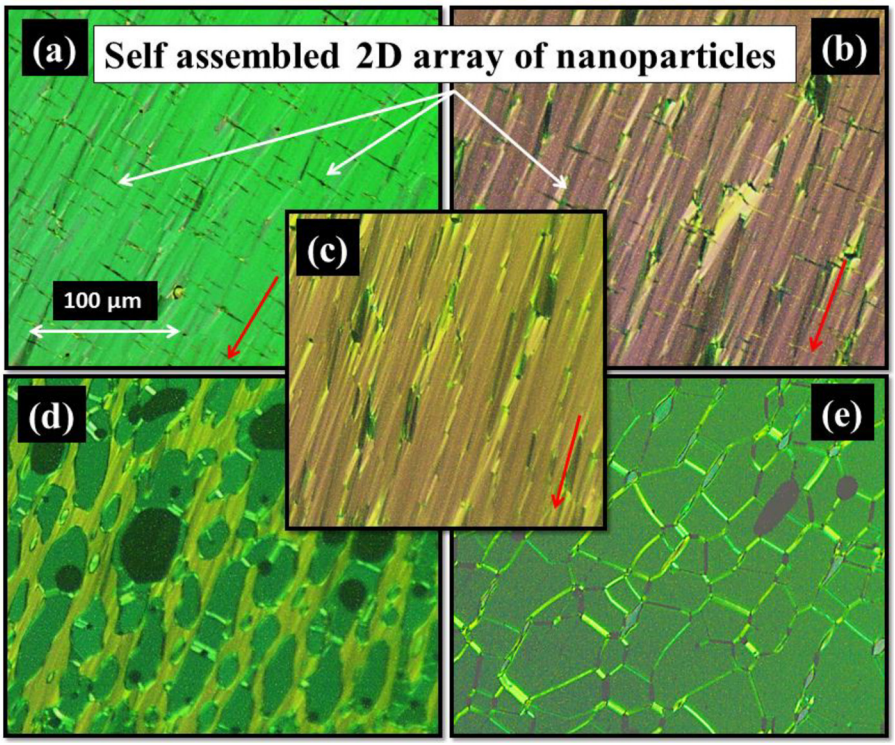

FIG. 5. Polarizing optical micrographs (under crossed polarizer-analyzer condition) of Mix.3 during the entire mesogenic phase. (a) In the deep SmC* phase (at 35 °C), (b) near transition from the SmC*-SmA phase (68 °C), (c) In the SmA phase (at 100 °C), (d) near transition from the SmA-N* phase (at 115 °C), and (e) In the N* phase (at 120 °C). The scale bar is the same for all the POMs and the red arrow represents the direction of rubbing.

aliphatic carbon chain of the NP ligand. In the direction of maintaining the minimum energy of the system, NPs tend to align side by side in between the smectic layers and form 2D array of nanoparticles, perpendicular to the direction of rubbing. The aligned texture of Mix.3 in SmC* phases consists a large number of such 2D arrays of nanoparticles. As can be seen from Fig. 5, these 2D arrays of NPs have been formed in almost whole volume of the dispersion. This shows that the high concentration of NPs causes a subsequent increase in the number of NP assemblies in the SmC* phase. These 2D arrays subsist even in the SmA phase [Fig. 4(b)]. It seems that for Mix.3, due to high concentration of NPs, a lesser correlation between the smectic layers results due to strong repulsive forces between the hydrophobic LC and hydrophobic ligands which in turn affect the polarizing ability of the system as discussed later in the manuscript. A similar result has been observed for a nanorod dispersed Liquid Crystal Polymer matrix and a Ps-*b*-PMMA/CdSe hybrid system.[33,49] The POMs of the chiral nematic phase for Mix.2 and Mix.3 show that the number of continuities increases as the concentration of NPs increases.

The POM image analysis gives an idea about the transition temperatures of a LC sample. We have found that the transition temperatures determined by the DSC study are very much in agreement with that observed by POM image analysis. Both the studies confirm the presence of the SmC* phase in spite of the formation of nanoparticle assemblies in Mix.2 and Mix.3, at room temperature. Here, it can be assumed that the LC molecules are less correlated due to the disconnections caused by NP assemblies but they still possess the smectic phase. In the SmC* phase, two coupling interactions are responsible for communicating tilt direction from layer to layer: the intralayer tilt coupling and interlayer tilt coupling. The aligned texture of the SmC* phase in between the two assemblies in the case of Mix.2 and Mix.3 indicates that the formation of assemblies is lowering the intralayer correlation between the LC molecules but the interlayer tilt coupling interaction is still there.

C. Dielectric relaxation analysis

The dielectric spectrum of the chiral smectic liquid crystal contains two significant collective relaxation processes, the Goldstone mode and Soft mode relaxation process. In the SmC* phase, the director is subjected to huge phase fluctuations with weak temperature dependency. The low frequency part contains absorption due to the collective phase fluctuations, which is the Goldstone mode (GM). The Goldstone mode is a thermally activated mode. It is easily observable in the planar orientation of the FLC molecules with the smectic layer perpendicular to the glass plates.[50]

The frequency dependence of the dielectric permittivity at four different temperatures of the SmC* phase [(a) at 35 °C, (b) at 50 °C, (c) at 70 °C, and (d) at 74 °C] is presented in Figs. 6(a), 6(b), 6(c), and 6(d). As discussed in the thermal analysis, the present FLC shows the SmC* phase until 72 °C. In accordance with that we can see that the value of relative permittivity (RP) is very high at low frequency until 70 °C for the FLC material. A high value of RP is due to the contribution of the goldstone mode. Though for Mix.1, we observe goldstone until 74 °C which might be due to the slight increase in SmC* phase-SmA phase transition temperature. It is very fascinating to observe goldstone mode in Mix.2 until 50 °C only and for Mix.3, we have not observed goldstone mode even at 35 °C. The non-appearance of Goldstone mode in the SmC* phase after a certain temperature shows that the presence of a self-assembled 2D array of nanoparticles affects the molecular fluctuations of the host FLC

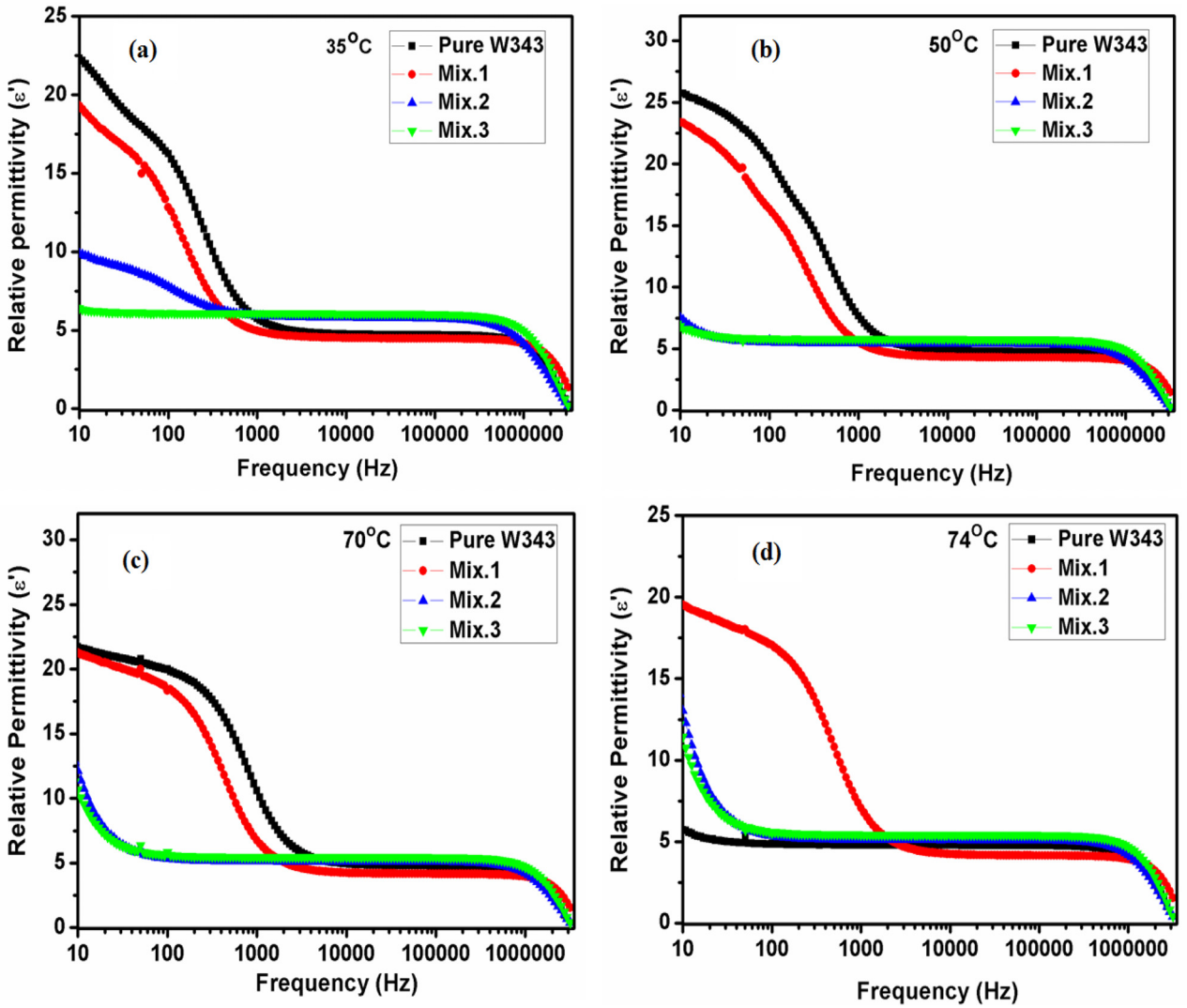

FIG. 6. Variation of relative permittivity (ε') with the variation in frequency for pure FLC (W343) and NP dispersed FLC composites at (a) 35 °C, (b) 50 °C, (c) 70 °C, and (d) 74 °C, respectively.

material. The non-appearance of GM can be attributed to any of the following two reasons: either SmC* phase has been supressed completely in the presence of assemblies of nanoparticles or the molecules are not able to follow the field due to the stabilizing (or freezing) effect of nanoparticle assemblies. As discussed earlier in the thermal and optical analysis, the SmC*-SmA phase transition temperatures for Mix.2 and Mix.3 are 70 °C and 69 °C, respectively. This shows that, even though the Mix.2 and Mix.3 are in the SmC* phase, the goldstone mode after a certain temperature cannot be observed. Relaxation behaviour of molecules in the SmC* phase for Mix.2 and Mix.3 can be understood by a representation of the formation of self-assembled 2D arrays of nanoparticles. Figure 7 shows a schematic of self-assembled 2D arrays of nanoparticles positioned perpendicular to the orientation of the LC molecular alignment in the planar aligned cell. In the SmC* phase, theses arrays disconnect the continuous helical arrangement of molecules. As observed in the POM images, these 2D arrays are aligned in between the smectic layers due to the mutual repulsive forces acting between the guest and host. The presence of these 2D arrays divides the composite system into domains and when the field is applied to the cell, these domains are polarized randomly leading to net polarization of the system to be very low. In Mix.2, one can see that these 2D arrays are larger in length and lesser in extent in comparison to the Mix.3. Therefore, it can be supposed that there is a better correlation between the smectic layers in Mix.2 as compared to Mix.3. Appearance of goldstone mode until 50 °C is the major consequence of the above assumption and due to the least correlation between the layers in Mix.3, we do not observe goldstone mode even at room temperature.

To confirm the non-appearance of a characteristic Goldstone mode in Mix.3, we have plotted the Tan Delta graph for pure and composite systems. All the dielectric modes can be easily visualized in the dielectric loss factor (tan delta) graph as shown in Fig. 8(a) at 35 °C, (b) at 50 °C, and (c) at 70 °C, respectively. A low frequency mode along with the Goldstone mode is observed in the case of pure FLC and Mix.1 at 35 °C. The ionic impurity contributes to the low frequency dielectric relaxations in an LC system in two separate ways—that is, from fast ions in the single-particle

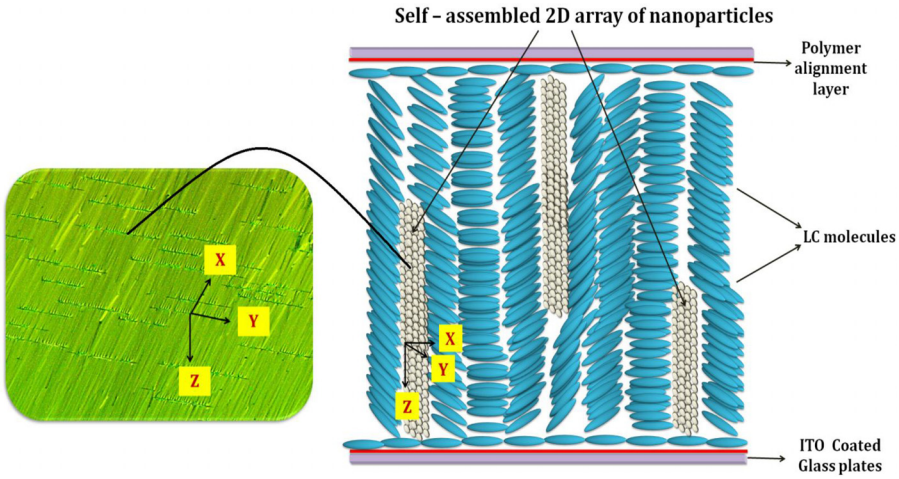

FIG. 7. Schematic illustration of the cross sectional view from the X-Z plane of the Silver NP dispersed FLC system showing 2 Dimensional (2D) arrays of nanoparticles between smectic layers. Disconnecting smectic layers with deformation of layers can be realized due to the 2D array of nanoparticles.

diffusion and slow ions in the ionization-recombination assisted diffusion. The appearance of a low frequency mode is attributed to the ionization-recombination assisted diffusion of slow ions in a planar alignment configuration.[51] This low frequency peak shifts to the higher frequency side on increasing the temperature and near SmC*-SmA phase transition temperature it merges with the Goldstone mode. Successively, the effect of silver nanoparticles on the nature of Goldstone mode and impurity linked relaxation can be seen in Fig. 8. The low frequency mode and Goldstone mode have been shifted to a lower frequency side with the increasing dopant concentration in the FLC. This suggests that the incorporation of NPs hinders the phase fluctuation in the azimuthal orientation of the molecular director. In the low-frequency limit, the shifting of impurity linked relaxation to the lower frequency side indicates that the presence of nanoparticles affects the ionization-recombination rate with the variable concentration of dopant. As discussed earlier, Mix.3 does not show goldstone mode even at very low temperatures and for Mix.2 goldstone mode disappears after 50 °C.

To visualize the effect of 2D arrays of nanoparticles on the migration of ionic charges in Mix.2 and Mix.3, we have calculated the DC conductivity of pure and silver nanoparticle dispersed FLC composites. DC conductivity is caused by the movement of free ionic charges present in LC medium under applied electric field. Figure 9 shows the conductivity value for pure and composite systems. It can be seen that for Mix.1, the DC conductivity value is almost similar to that of the pure FLC material. However, it has increased significantly for the Mix.2 and Mix.3 as compared to pure FLC. This increase is more prominent at high temperature where ionic charges have sufficient energy to move between electrodes. This indicates that an presence of 2D arrays of nanoparticles is providing an easy path (or conductive path) for the migration of impurity charge carriers from one electrode to another. As a result, material ability to allow the transport of ionic charge carriers increases, drastically. A very small

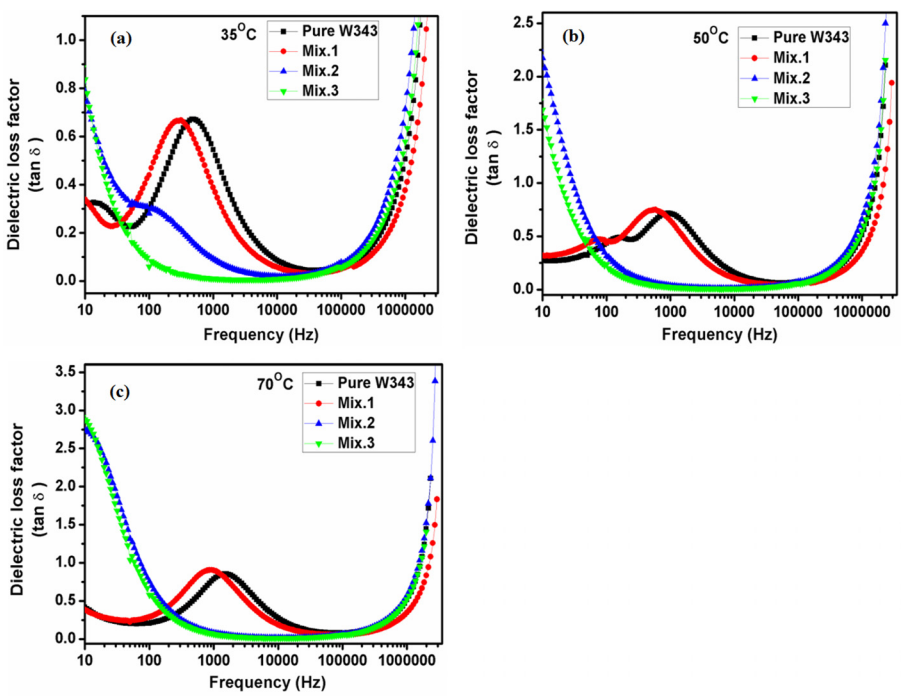

FIG. 8. Behavior of dielectric loss factor (tan δ) of pure FLC (W343) and NP dispersed FLC composites with frequency at (a) 35 °C, (b) 50 °C, and (c) 70 °C.

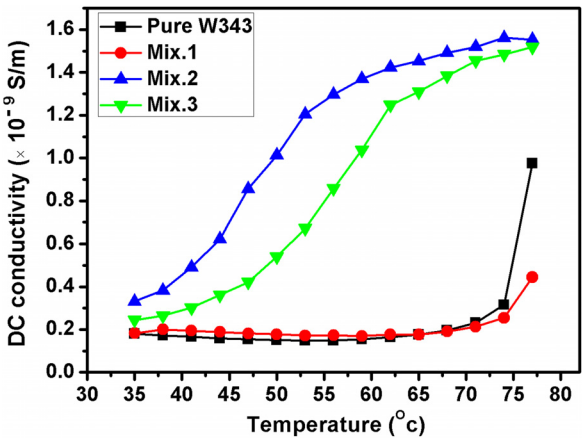

FIG. 9. DC conductivity of pure FLC (W343) and silver nanoparticle dispersed FLC composites as a function of temperature.

decrement in the conductivity value has been observed while increasing the concentration from 0.3 wt./wt. % to 0.5 wt./wt. %. As observed in the POMs of Mix.3, system has now divided into so many small domains that might be hindering the movement of ionic charges between the electrodes.

D. Electro–optical parameter analysis

Nanoparticle induced changes in alignment and low polarizing ability of the molecules in composites (Mix.2 and Mix.3) have been verified by the analysis of electro-optical parameters. We have performed the E-O (electro-optical) measurements for all the samples under consideration. The voltage dependent analysis of spontaneous polarization, optical tilt angle, and response time for the pure FLC, Mix.1, and Mix.2 is presented in Figs. 10(a), 10(b), and 10(c) at 35 °C. As discussed previously, for Mix.3, all these parameters cannot be measured due to insignificant polarization of the molecules in the presence of the 2D arrays of nanoparticles. The presence of any guest entity and change in the component percentage (in the case of a multicomponent FLC material) can sufficiently influence the spontaneous polarization and optical tilt angle value of the pristine FLC material.[52,53] Figure 10(a) shows the behaviour of spontaneous polarization (Ps) with the applied electric field. In the SmC* phase due to the tilted geometry of the molecules, mirror symmetry gets broken and a definite value of spontaneous polarization can be achieved after removing the helical structure by surface anchoring or electric field. In the present

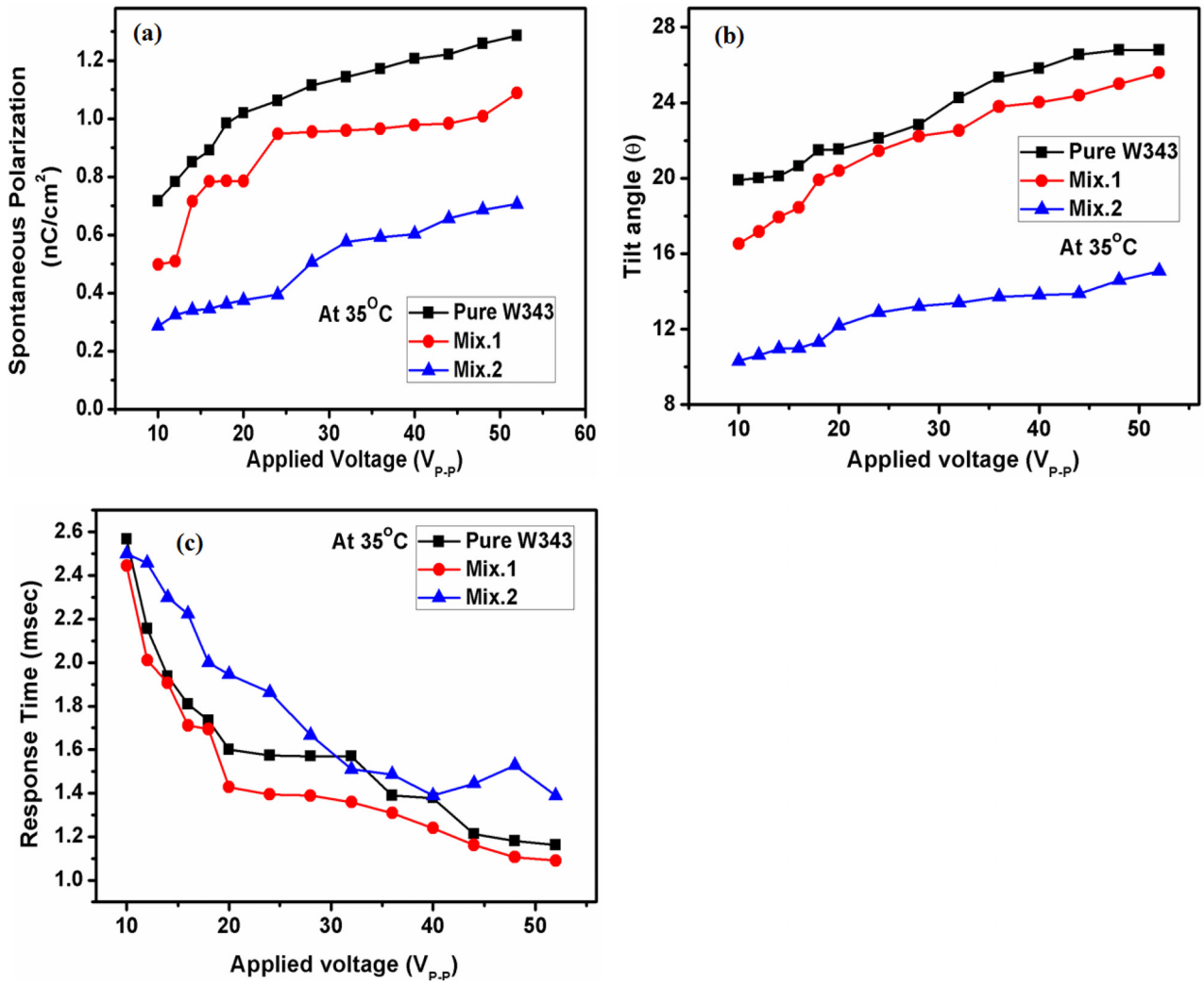

FIG. 10. Behavior of material parameters of pure FLC (W343) and NP dispersed FLC composites; (a) Spontaneous polarization, (b) Optical tilt angle, and (c) Response time with the variation in applied voltage at room temperature (at 35 °C).

study, the modifications in the Ps value of the FLC material and composites can be understood by taking into account the two different reasons. First, the correlation between the dipole moments of nanoparticles and FLC molecules and second is the polarizing ability of composites. For Mix.1, the lower Ps values are attributed to the antiparallel correlation of dipole moments of the hexanethiol capped silver nanoparticles and FLC molecules. One can see that antiparallel correlation is less effective at this dopant concentration. As the number of FLC dipoles per unit volume could be more or less similar to the non-dispersed FLC material, hence affecting Ps very less.[54] However for Mix.2 and Mix.3, the scenario changes drastically. As the dispersion of nanoparticles has led to the formation of 2D arrays of nanoparticles, one cannot talk about the correlation between the dipole moments of two (guest and the host). A lower Ps value in the case of Mix.2 is due to the formation of domains separated by these 2D arrays. These domains will be randomly oriented due to the restriction imposed by the 2D arrays of nanoparticles in the presence of applied field. Therefore, the Ps vector will also be oriented in the different direction and will cause a lower measurable value for Mix.2. As in Mix.3, the whole volume of the dispersion is divided into several small domains separated by these arrays; the overall measurable Ps value becomes very low (or becomes non-measurable).

The comparative optical tilt angle values of pure FLC show that it is following the general increasing trend [Fig. 10(b)] and gets saturated at a certain voltage. However for composites, a saturated value could not be achieved. The silver nanoparticle dispersed composite shows a low optical tilt angle with the following trend $\theta_{\text{Pure}} \sim \theta_{\text{Mix.1}} > \theta_{\text{Mix.2}}$. A very slight change in the optical tilt angle value for Mix.1 might be due to the alignment changes after the dispersion of NPs. However, a noteworthy decrease in the optical tilt angle value for Mix.2 is a confirmation of the lower polarizing ability of the composites. Due to the lesser correlation between the smectic layers, the molecules are not able to follow the field direction. As the molecules do not achieve their max conical position on two sides, actual tilt angle values cannot be acquired. And the apparent optical tilt angle value for Mix.2 is found to be lowest among FLC materials and Mix.1. The non measurable value of the apparent optical tilt angle for Mix.3 indicates that the molecules get freeze between different domains separated by 2D arrays of NPs causing no switching.

An expeditious optical response for Mix.1 in comparison to that of pure can be observed in Fig. 10(c). The response time of the FLC is inversely proportional to the anchoring energy[55] and enhancement in the same results in the form of fast response time for Mix.1. However, longer response time in the case of Mix.2 indicates that in the presence of 2D arrays of nanoparticles, FLC molecules are not able to rapidly follow the field.

IV. CONCLUSIONS

The hexanethiol capped metallic silver nanoparticles are used as a dopant in the multicomponent Ferroelectric Liquid Crystal mixture (FLC-W343), in the present study. To determine the importance and role of these silver NPs in the FLC, thermal, dielectric, and electro-optical measurements have been performed. The phase transition temperatures are found to be affected by varying the concentration of silver nanoparticles. Optical image analysis has shown that the dispersion of NPs affects the alignment of LC molecules in the respective phase. Due to the strong repulsive forces acting between the host and guest nanoparticle, the formation of self-assembled 2D arrays of nanoparticles in the direction perpendicular to the rubbing occurs in the composites with high dopant concentration. These 2D arrays cause the non-appearance of goldstone mode in the relaxation behavior of Mix.2 and Mix.3. Various other parameters, i.e., DC conductivity, spontaneous polarization, and apparent optical tilt angle, have also been changed in the presence of these 2D arrays of nanoparticles. This comprehensive study reveals the importance of concentration of the guest entity into the host LC material, as it can affect the molecular alignment and various other LC parameters, drastically. Such a combination of the metallic NPs and FLC material provides a better understanding towards the development of novel materials for different applications.

ACKNOWLEDGMENTS

Author TV is thankful to UGC, New Delhi for providing financial assistance in the form of UGC-BSR Fellowship [F.4-1/2006(BSR)/7-177/2007(BSR)]. S.K.G. is thankful to SERB India for providing fellowship under the young scientist scheme (YSS/2015/000367). The authors are also grateful to DST for the grant of funds in the form of INDOPOLISH project. R.M. is thankful to UGC for grant of research award (2014–16) and mid-career research award 2017.

[1]A. L. Porter and J. Youtie, J. Nanopart. Res. **11**, 1023 (2009).
[2]F. Rosei, J. Phys.: Condens. Matter **16**, S1373 (2004).
[3]P. Goel, P. L. Upadhyay, and A. M. Biradar, Liq. Cryst. **40**, 45 (2013).
[4]P. Kumar, A. Kishore, and A. Sinha, Adv. Mater. Lett. **7**, 104 (2016).
[5]H. K. Bisoyi and S. Kumar, Chem. Soc. Rev. **40**, 306 (2011).
[6]H. Qi and T. Hegmann, Liq. Cryst. Today **20**, 102 (2011).
[7]A. Rudzki, R. Evans, G. Cook, and W. Haase, Appl. Opt. **52**, E6 (2013).
[8]M. Inam, G. Singh, A. M. Biradar, and D. S. Mehta, AIP Adv. **1**, 042162 (2011).
[9]S. Pandey, S. K. Gupta, D. P. Singh, T. Vimal, P. K. Tripathi, A. Srivastava, and R. Manohar, Polym. Eng. Sci. **55**, 414 (2015).
[10]J. Jadzyn, Liq. Cryst. **26**, 453 (1999).
[11]R. Manohar, S. Manohar, and V. S. Chandel, Mater. Sci. Appl. **2**, 839 (2011).
[12]L. Dolgov, O. Yaroshchuk, S. Tomyuko *et al.*, Condens. Matter Phys. **15**, 33401 (2012).
[13]I. Dierking, G. Scalia, and P. Morales, J. Appl. Phys. **97**, 044309 (2005).
[14]S. Sridevi, S. K. Prasad, G. G. Nair, V. D'Britto, and B. L. V. Prasad, Appl. Phys. Lett. **97**, 151913 (2010).
[15]A. Chandran, J. Prakash, J. Gangwar, T. Joshi, A. K. Srivastava, D. Haranath, and A. M. Biradar, RSC Adv. **6**, 53873 (2016).
[16]T. Matsushita, J. Masuda, T. Iwamoto, and N. Toshima, Chem. Lett. **36**, 1264 (2007).
[17]S. K. Prasad, K. L. Sandhya, G. N. Geetha, S. H. Uma, C. V. Yelamaggad, and S. Sampath, Liq. Cryst. **33**, 1121 (2006).
[18]A. S. Pandey, R. Dhar, S. Kumar, and R. Dabrowski, Liq. Cryst. **38**, 115 (2011).
[19]U. Kreibig and M. Vollmer, *Springer Series in Materials Science* Vol. 25 (Springer-Verlag, Berlin, Heidelberg, 1995).

[20]S. K. Ghosh, S. Nath, S. Kundu, K. Esumi, and T. Pal, J. Phys. Chem. B **108**, 13963 (2004).
[21]K. Saumyakanti, M. Pramit, C. Wei-Shun, T. Alexei, F. Eric, R. Z. Eugene, and L. Stephan, J. Phys. Chem. C **114**, 7251 (2010).
[22]J. Prakash, A. Choudhary, A. Kumar, D. S. Mehta, and A. M. Biradar, Appl. Phys. Lett. **93**, 112904 (2008).
[23]A. Kumar, G. Singh, T. Joshi, G. K. Rao, A. K. Singh, and A. M. Biradar, Appl. Phys. Lett. **100**, 054102 (2012).
[24]K. K. Vardanyan, E. D. Palazzo, and R. D. Walton, Liq. Cryst. **38**, 709 (2011).
[25]K. K. Vardanyan, R. D. Walton, and D. M. Bubb, Liq. Cryst. **38**, 1279 (2011).
[26]P. Yaduvanshi, A. Mishra, S. Kumar, and R. Dhara, Liq. Cryst. **42**, 1478 (2015).
[27]P. Schwerdtfeger, Angew. Chem., Int. Ed. **42**, 1892 (2003).
[28]U. B. Singh, R. Dhar, R. Dabrowski, and M. B. Pandey, Liq. Cryst. **40**, 774 (2013).
[29]M. Mishra, R. S. Dabrowski, J. K. Vij, A. Mishra, and R. Dhar, Liq. Cryst. **42**, 1580 (2015).
[30]P. Ganguly, A. Kumar, S. Tripathi, D. Haranath, and A. M. Biradar, Appl. Phys. Lett. **102**, 222902 (2013).
[31]J. I. Fukuda, J. Phys. Soc. Jpn. **78**, 041003 (2009).
[32]K. J. Stebe, E. Lewandowski, and M. Ghosh, Science **325**, 159 (2009).
[33]T. Du, J. Schneider, A. K. Srivastava, A. S. Susha, V. G. Chigrinov, H. S. Kwok, and A. L. Rogach, ACS Nano **9**(11), 11049 (2015).
[34]A. N. Gowda, M. Kumar, A. R. Thomas, R. Philip, and S. Kumar, Chem. Sel. **1**, 1361 (2016).
[35]T. Vimal, S. Pandey, S. K. Gupta, D. P. Singh, and R. Manohar, J. Mol. Liq. **204**, 21 (2015).
[36]S. Dumrongrattana, C. C. Huang, G. Nounesis, S. C. Lien, and J. M. Viner, Phys. Rev. A **34**, 5010 (1986).
[37]S. Pandey, T. Vimal, D. P. Singh, S. K. Gupta, P. Tripathi, C. Phadnis, S. Mahamuni, A. Shrivastava, and R. Manohar, Liq. Cryst. **41**, 1811 (2014).
[38]M. Subrao, D. M. Potukuchi, G. S. Ramachadra, P. Bhagavath, S. G. Bhat, and S. Maddasani, Belistein J. Org. Chem. **11**, 233 (2015).
[39]M. B. Pandey, R. Dhar, V. K. Agrawal, R. P. Khare, and R. Dabrowski, Phase Trans. **76**, 945 (2003).
[40]S. S. Sastry, B. G. S. Rao, K. B. Mahalakshmi, K. Mallika, C. N. Rao, and H. S. Tiong, Condensed Matter Phys. **2012**, 423650 (2012).
[41]N. Sood, S. Khosla, D. Singh, and S. S. Bawa, J. Inf. Disp. **12**, 129 (2011).
[42]S. Singh, *Liquid Crystal Fundamentals* (World Scientific, Singapore, 2002).
[43]A. Roshi, G. S. Iannacchione, P. S. Clegg, and R. J. Birgeneau, Phys. Rev. E **69**, 031703 (2004).
[44]H. Duran, B. Gazdecki, A. Yamashita, and T. Kyu, Liq. Cryst. **32**, 815 (2005).
[45]L. M. Lopatina and J. V. Selinger, Phys. Rev. Lett. **102**, 197802 (2009).
[46]G. W. Gray and J. W. G. Goodby, *Smectic Liquid Crystals: Textures and Structures* (Leonard Hill, Glasgow, 1984).
[47]V. Tomar, T. F. Roberts, N. L. Abbott, J. P. Hernández-Ortiz, and J. J. De Pablo, Langmuir **28**, 6124 (2012).
[48]J. C. Biffinger, H. W. Kim, and S. G. Dimagno, ChemBioChem **5**, 622 (2004).
[49]E. Ploshnik, A. Salant, U. Banin, and R. Shenhar, Adv. Mater. **22**, 2774 (2010).
[50]G. Durand and P. Martinot-Lagarde, Ferroelectrics **24**, 89 (1980).
[51]M. Y. Jin and J. J. Kim, J. Phys.: Condens. Matter **13**, 4435 (2001).
[52]M. Tykarskaa, R. Dabrowski, M. Czerwinski, A. Chelstowska, W. Piecek, and P. Morawiak, Phase Trans. **85**, 364 (2012).
[53]S. Tripathi, P. Ganguly, D. Haranath, W. Haase, and A. M. Biradar, Appl. Phys. Lett. **102**, 063115 (2013).
[54]R. K. Shukla, X. Feng, S. Umadevi, T. Hegmann, and W. Haase, Chem. Phys. Lett. **599**, 80 (2014).
[55]T. Sako, N. Itoh, A. Sakaigawa, and M. Koden, Appl. Phys. Lett. **71**, 461 (1997).